

PROPOSAL OF THE REFLECTION HARD X-RAY SELF-SEEDING AT THE SHINE PROJECT *

Tao Liu[†], Chao Feng[‡],

Shanghai Advanced Research Institute, Chinese Academy of Sciences, Shanghai 201210, China

Abstract

FEL self-seeding has been demonstrated a great advantage for the generation of a fully coherent and high brightness X-ray pulse experimentally. Generally, transmission monochromators with single crystal are adopted worldwide, such as LCLS, PAL-XFEL and European-XFEL. Recently, the self-seeding scheme based on a reflection monochromator with a double-crystal is proposed and demonstrated at SACLA successfully. In view of several potential advantages of the reflection type, here we give the proposal of the reflection monochromator based self-seeding and enable the application on the SHINE project. This manuscript is mainly focus on monochromator schemes at SHINE, instead of FEL simulations. We will present considerable schemes based on the specific undulator line.

INTRODUCTION

A crystal monochromator is usually used on the beam line of a light source for the achievement of a coherent hard X-ray, which will be transport to the user experiment. The conventional monochromator based on Bragg or Laue diffraction (reflection) consists of double crystals or four crystals and the consequent time delay is generally centimetre-scale. Therefore, it is impracticable for hard X-ray self-seeding that a centimetre-scale time delay requires temporal overlap with a chicane with dozens of meters long.

The normal method of hard X-ray self-seeding is based on a transmission monochromator with a single crystal, which is about $100\ \mu\text{m}$ thick and the efficient wake delay is in the $10\ \mu\text{m}$ level [1]. Such time delay is suitable for a small chicane between two undulator sections. Currently, it has been demonstrated successfully at LCLS [2] and PAL-XFEL, and European-XFEL is also in preparation. However, there are several disadvantages that the monochromatic efficiency is relatively low (0.1%), the heat-loading problem of the crystal is relatively heavy and the processing technology of the crystal ($100\ \mu\text{m}$ thick) is quite challenging. Besides, the transmission monochromator usually use the large incidence angle ($\pi/4 - \pi/2$), resulting in a small-scale and lower-energy photon energy coverage.

Recently, a channel-cut crystal monochromator was proposed based on the Bragg reflection with a slit gap of $90\ \mu\text{m}$ and did experiment successfully at SACLA [3]. This reflection monochromator induces a time delay about $100\ \mu\text{m}$ level which is feasible for a 4 meter long chicane. Comparing

to the transmission monochromator, the reflection one has the following major advantages. First, its monochromatic efficiency is 1 – 2 order of magnitude higher than the transmission one. Second, the heat-loading effect is smaller than the transmission one, which might be easy for the cooling system. Third, the signal-to-noise ratio is better that only the monochromatic pulse is injected into the following undulator, instead of the transmission one with a powerful SASE signal at the head of the pulse. Fourth, the processing technology is relatively easier than the transmission one. Furthermore, the reflection monochromator can use the small incidence angle, and it can cover higher energy photon.

In the previous paper [4], we have proposed a transmission scheme based on the SHINE project. In this manuscript, we discuss the reflection monochromator based on the SHINE project. SHINE, Shanghai High Repetition Rate XFEL and Extreme Light Facility consists of 3 undulators lines, and self-seeding scheme is the basic scheme for each line. The lines FEL1 will cover photon energy range of 5-13 keV by the normal undulator and FEL3 will cover the range of 10-15 keV by the superconducting undulator.

SCHEME PROPOSAL

Double-Crystal Monochromator

The basic double-crystal monochromator is shown in Fig. 1, where the layout consists of two crystals and a beam stopper. Mechanically, the so-called two crystals are not two individual crystals but a channel-cut crystal. The beam stopper is pressed against the right edge of the first crystal which is used to block the SASE pulse transmitting the crystal.

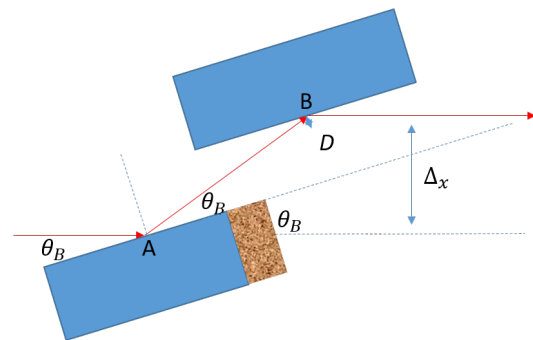


Figure 1: Reflection monochromator with double-crystal for self-seeding.

The monochromator will induce a time delay $\Delta\tau$ and a transverse offset Δx . The slit gap D is assumed as $100\ \mu\text{m}$, then $\Delta\tau$ and Δx can be calculated as

$$\Delta\tau = \frac{D}{c \sin \theta_B} (1 - \cos 2\theta_B) \quad (1)$$

* Work supported by the National Natural Science Foundation of China Grant No. 11605277

[†] liutao@zjlab.org.cn; liutao@sinap.ac.cn

[‡] fengchao@zjlab.org.cn

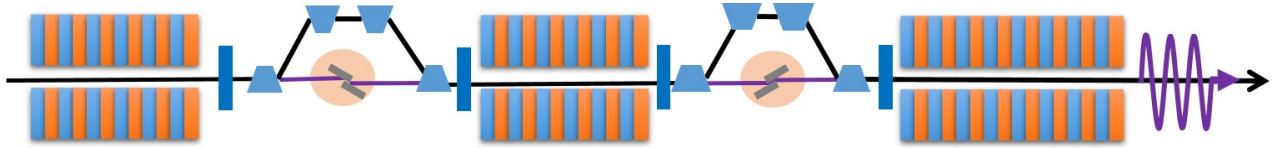


Figure 2: Layout of the two-stage reflection hard X-ray self-seeding scheme at the SHINE.

$$\Delta x = 2D \cos \theta_B \quad (2)$$

where c is velocity of light and θ_B is Bragg angle. As the example of C111 symmetric diamond crystal, one can get time delay and transverse offset with respect to Bragg angle listed in Table 1. When the Bragg angle $\theta_B > 37^\circ$, i.e. $E_{pho} < 5$ keV, the time delay will be more than $100 \mu\text{m}$, the transverse offset will cover $17\text{-}160 \mu\text{m}$. Besides, for a relatively large Bragg angle, the processing technology of the edge of crystal will be more challenging. Consequently, we mainly consider relatively small angle which is still enough to cover $5\text{-}13$ keV of FEL1. The time delay is easy for a small chicane, however, the transverse offset will impact on FEL gain though a couple of correctors are large enough to compensate the transverse offset. FEL simulations by Genesis [5] are presented in Fig 3 and Fig. 4 with different transverse offset from the central magnetic field plane. Figure 3 shows the peak power evolutions which indicate that the offset larger than $40 \mu\text{m}$ is infeasible for FEL gain. Figure 4 shows the deviation of the beam centre along the long undulator that clarifies the reason of FEL degradation.

Table 1: Time Delay and Transverse Offset with Respect to Bragg Angle for C111

E_{pho} (keV)	θ_B (deg)	$c\Delta\tau$ (m)	Δx (m)
3.023	85.0	199.2	17.4
3.20	70.0	187.9	68.4
5.0	37.0	120.4	159.7
7.0	25.5	86.1	180.5
15.0	11.6	40.2	195.9
25.0	6.9	24.0	198.6

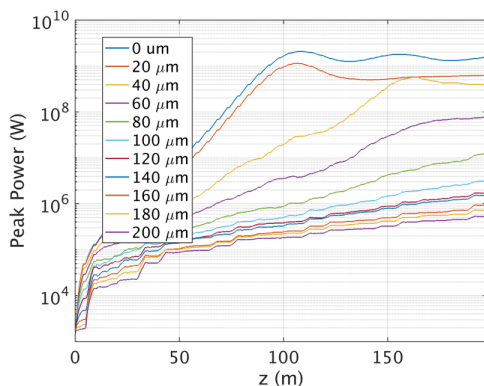


Figure 3: Self-seeding peak power with respect to the undulator length z with different offset of y .

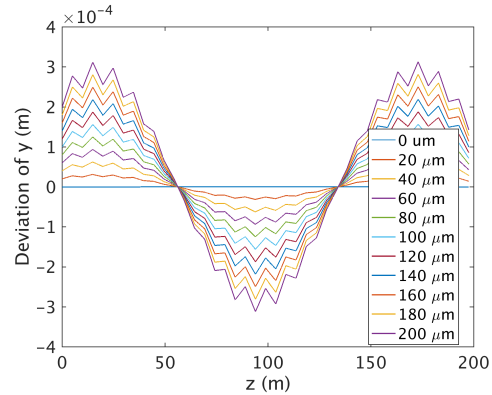


Figure 4: Deviation of y with respect to the undulator z length with different offset of y .

Feasible Schemes

It is clear that the beam offset from magnetic field central plane of undulators impacts on FEL gain significantly. There are several feasible methods to resolve this issue.

- First, moving the magnetic field centre of the undulator downstream. Usually, we consider using gap-adjustable planar undulator, which has been used in the Line FEL1 of SHINE. As shown in Fig. 2, a cascaded reflection self-seeding scheme includes two monochromators with opposite directions. The magnetic field centre of the second undulator section will be adjusted according to the beam offset. The second monochromator with opposite direction can make the trajectory back to the initial one. However, this method does not work on the gap-fixed undulator.
- Second, adopting two double-crystals in a monochromator. This method can cancel the transverse offset efficiently, and yet double the time delay. Certainly, the time delay is still achievable for the inter-section chicane. These two double-crystals are placed symmetrically in a same monochromator, but independent adjustable. This method is feasible for FEL self-seeding, where the challenging aspect is manufacture process and adjustment accuracy. It applies suitable for the Line FEL3 of SHINE with superconducting undulator.
- Third, using p-polarized reflection. Generally, s-polarized reflection (or transmission) is used in normal monochromator since the reflectivity of the s-polarization is larger than the p-polarization one and even the p-polarization reflectivity drops to zero when being incident on an interface at Brewster's angle. Nevertheless, the reflectivity of the p-polarization is still

the same order of the reflectivity of the s-polarization as long as the incidence is far from Brewster's angle, which is much larger than the efficiency of the transmission case. For an planar undulator, the plane perpendicular to the magnetic field has the same magnetic field and high tolerance for beam position. This method is quite considerable for self-seeding to avoid the vertical offset.

Parameter Choice

Similar to the previous transmission scheme [4], the diamond crystal is still preferred due to the heat-loading strength. But in view of the processing technology, silicon (Si) crystal might be easier than diamond (C) crystal, and it is also worthy of consideration. Both of these two category can cover the photon energy range from 5-15 keV.

the reflection power of C400 is lower than the C111 one, but with better coherence. In spite of several spikes of C111, the bandwidth is still smaller than FEL gain dependent bandwidth, which can be amplified next undulator section. For a cascaded case, the first stage with C111 and the second with C400 are possible ensuring a narrow bandwidth pulse and low heat-loading of crystal. It is worth noting that the smaller Bragg angle, more challenging for processing technology. Once insufficient accuracy of the crystal, the mono pulse can not be achievable. For p-polarized reflection case, the Brewster's angle is 4.2 keV for C111 and 9.8 keV for C400, it has to adopt the other lattice around these photon energy. As an example of Line FEL3 with photon energy of 10-15 keV, the range of lattice C220 should be 19°-29° which would be better C400.

CONCLUSION

In this manuscript, we introduce the application of the reflection monochromator on the SHINE project, and present the proposal to solve several important issues briefly. Three methods concluding undulator moving, two double-crystals and p-polarized reflection are proposed, respectively. Particularly, the Line FEL3 is worth to consider the p-polarized reflection case due to the superconducting undulator with fixed gap. In details, the crystal lattice should be chosen based on the specific monochromator case and photon energy. It is a preliminary proposal of reflection hard X-ray self-seeding at the SHINE project, and many advanced work will be done next.

ACKNOWLEDGEMENTS

The authors would like to thank for Bo Liu, Haixiao Deng, Dong Wang, Hanghua Xu and Xiaohao Dong for helpful discussions and useful comments.

REFERENCES

- [1] G. Geloni, V. Kocharyan, and E. L. Saldin, "A novel selfseeding scheme for hard x-ray FELs", *Journal of Modern Optics*, vol. 58, issue 16, p. 1391, (2011).
- [2] J. Amann *et al.*, "Demonstration of self-seeding in a hard-X-ray free-electron laser", *Nature Photonics*, 6, 693-698 (2012).
- [3] I. Inoue *et al.*, "Generation of narrow-band X-ray free-electron laser via reflection self-seeding", *Nature Photonics*, 13, 319-322 (2019).
- [4] T. Liu *et al.*, "Optimization for the Two-Stage Hard X-Ray Self-Seeding Scheme at the SCLF", in Proc. *9th International Particle Accelerator Conference (IPAC2018)*, Vancouver, BC, Canada, Apr.-May 2018, pp. 4460-4463. doi.org/10.18429/JACoW-IPAC2018-THPMK070
- [5] S. Reiche, "GENESIS 1.3: a fully 3D time-dependent FEL simulation code", *Nucl. Instrum. Methods Phys. Res. A*, vol. 429, issue 1-3, p. 243, (1999).
- [6] ESRF, X-ray Oriented Programs Software Package. <https://www.aps.anl.gov/Science/Scientific-Software/XOP>

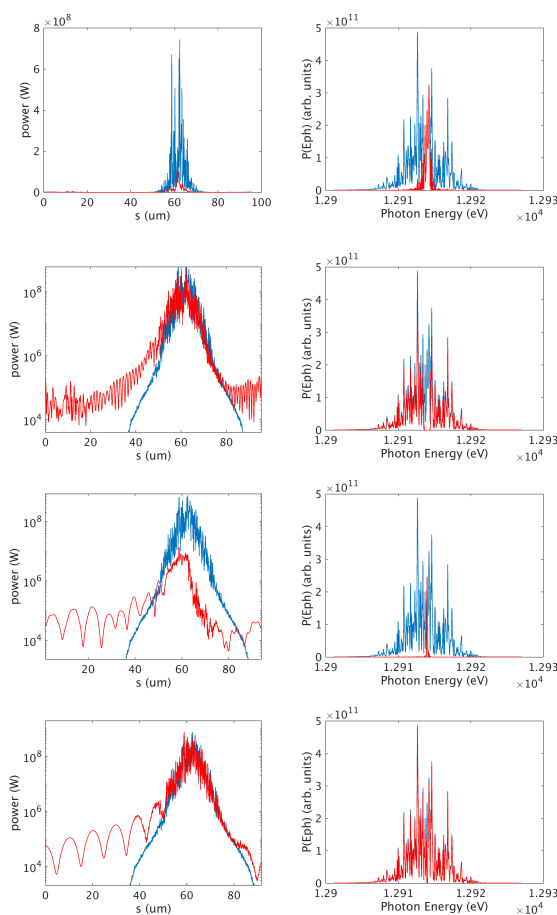


Figure 5: FEL radiation before (blue) and after (red) monochromator. Top-to-bottom: reflection by C111, transmission by C111, reflection by C400 and transmission by C400. Left: pulse power, right: Spectrum.

Figure 5 shows the 13 keV FEL pulses and spectra before (blue) and after (red) diamond crystal monochromators with different lattices. The code XOP2.4 is used here [6]. For comparison, the transmission results are also presented here. For C111 and C400, the reflection power is much higher than the wake power of transmission. In view of reflection,

Content from this work may be used under the terms of the CC BY 3.0 licence (© 2019). Any distribution of this work must maintain attribution to the author(s), title of the work, publisher, and DOI